



THE SOLUTION OF AEROELASTIC PROBLEMS WITHIN THE
FRAME OF TRIDIMENSIONAL UNSTEADY AERODYNAMIC PANEL METHOD.

A. Frediani, L. Polito, A. Salvetti
Dipartimento di Ingegneria Aerospaziale
Via Diotisalvi, 2 - 56100 - Pisa - Italia

Yates thinks this is good

Abstract

This paper deals with how to solve the flutter problem by a tridimensional unsteady panel method; both cubic splines and Padè approximation are used to interpolate aerodynamic forces.

Flutter speed is assessed by means of an automated solution based on the procedure of following any single flutter mode when speed increases. Examples of application are discussed.

I. Introduction

Flutter phenomena, as is well known, consist of dynamic self-excited instability where lifting surfaces absorb energy from the airstream; flutter is likely to occur in modern aircraft because of increased flexibility, high velocities and the presence of a wide variety of wing-suspended loads.

Several methods for solving flutter problems exist; the ability to give accurate flutter prediction on speed and frequency depends greatly on the aerodynamic model which is used. Efficient numerical methods of calculating aerodynamic forces have recently been proposed; their utilization in flutter prediction seems to be of considerable interest from the point of view of accuracy, time consumption and the possibility of taking the aerodynamics of suspended bodies, etc, into account.

In this paper, a method for calculating the aerodynamic potential field is considered; in this method the integral equation of motion is solved in terms of the limit value of the velocity potential function on the body surface, in accordance to the Morino formulation, instead of resorting to direct application of the boundary conditions.

This method is simple and a limited number of panels is necessary in order to take the main aerodynamic effects into account; moreover, interesting applications in flutter suppression and control are permitted.

The flutter solution proposed in this paper is based on the procedure, which is well known, as can be seen from the litera-

ture, of following the evolution of any single flutter mode when velocity increases up to the critical flutter condition.

A computer program has been worked out to solve flutter problems in the context described above; a flow chart in this connection is to be found in fig. 1.

The main features of this program and, in particular, the aerodynamic operator and the procedure for solving the problem of flutter will be examined in the rest of the paper.

II. The flutter problem and methods of solution

The equation of an elastic system in motion in a fluid stream, when "n" generalized coordinates, $\{q(t)\}$, are considered, can be written in the general form

$$1) \quad [M] \{\ddot{q}(t)\} + [C] \{\dot{q}(t)\} + [K] \{q(t)\} = \{F_a\}$$

where:

$[M]$, $[C]$ and $[K]$ are generalized matrices defining the inertial, damping and elastic properties of the system;

$\{F_a\}$ is the vector of the generalized aerodynamic forces. When the modulus of the asymptotic speed, V , equals that of critical flutter, motion is harmonically self-excited, that is

$$2) \quad \{q(t)\} = \{q\} e^{i\omega t}$$

where ω is the circular frequency and "i" and "t" indicate, respectively, the imaginary unit and the time variable; in more general terms, damped or amplified vibrations of the type

$$2.a) \quad \{q(t)\} = \{q\} e^{pt},$$

where p is a complex number, are considered and, consequently, the expression of the aerodynamic forces becomes

$$3) \quad \{F_a\} = \frac{\rho_\infty V^2}{2} [A] \{q\} e^{pt},$$

where ρ_∞ is the undisturbed flow density and the elements of the matrix $[A]$ depend on the Mach number, M , and the reduced frequency,

$$k = \frac{\omega c}{V}, \quad (c \text{ is a reference length and } V \text{ is the asymptotic speed}).$$

The equations of the motion become, then,

$$4) \quad [F] \{q\} = \{0\}$$

where

$$4.a) \quad [F] = [M] p^2 + [C] p + [K] - \frac{\rho_\infty V^2}{2} [A].$$

The methods for the solution of (4) depend on the model of aerodynamics which is used.

In the case of quasisteady (or simple forms of unsteady) aerodynamics, where it

can be put $[A] = [A_0] + [A_1] p$, the relationship (4.a) defines a polynomial in p with real coefficients (aerodynamic matrices $[A_0]$ and $[A_1]$ are real); for assigned values of speed and density the equation $\det [F] = 0$ gives rise to conjugate complex roots, $p = \gamma k \pm ik$, where γ is interpreted as the rate of the amplitude decay of two successive cycles; this well-known method is named "p-method".

When more sophisticated formulations of the aerodynamics are required to study effective configurations, as in the case of panel methods (which are of interest in the present paper), the aerodynamic matrices are available only for harmonic motions ($p = ik$) and the elements of these matrices are complex numbers which depend on k and M .

Three methods seem particularly interesting in the literature, namely: the "k-method", the "p-k method" and direct solution of the problem as non-linear system (/1/, /2/).

In the "k-method", the flutter equation is written in the form (/3/):

$$5) \quad \left[\frac{1}{c^2} [M] k^2 + \frac{1}{V^2} [K] - \frac{1}{2} \rho_\infty [A(ik, M)] \right] \{q\} = \{0\};$$

at selected values of k , M and ρ_∞ , the values of $1/V^2$ which solve (5) (real or complex) can be obtained as solutions of an eigenvalue problem and expressed in the form:

$$\frac{1}{V^2} (1 + ig); \quad \text{the term } ig [K] \{q\} \text{ is interpreted as an hysteresis damping and, then, the flutter speed corresponds to the condition: } g = 0.$$

The "k-method" was not implemented in the present computer program shown in fig. 1 owing to some disadvantages of the method, regarding:

The "k-method" was not implemented in the present computer program shown in fig. 1 owing to some disadvantages of the method, regarding:

- a) the interpretation of the frequency-speed and damping-speed plots;
- b) the impossibility of assessing flutter by relating the values of ρ_∞ , M and V by means of, e.g., the ISA (International Standard Air); in fact, should ρ_∞ and M be fixed, the speed would be given as $V = Ma = M f(\rho_\infty)$, where the speed of the sound, a , is a known function of ρ_∞ according to the ISA, without being solution of the problem (5);
- c) it is quite difficult, in general, to distinguish any single aeroelastic mode in the speed-damping plane because the order of extraction of the eigenvalues is not always the same when the eigenvalue problem is solved for the different values of k ; thus, the aeroelastic mode becoming critical is unknown and no indication is available on possible modifications of the structure.

In the "p-k method" the flutter problem is written in the form.

$$6) \quad \left[\frac{V^2}{c^2} [M] p^2 + [K] - \frac{1}{2} \rho_\infty V^2 [A(ik, M)] \right] \{q\} = \{0\}$$

or in a more generalized form (/3/) including e.g., artificial viscous dampings, the effects of controls, the presence of an hysteresis damping, etc.

It transpires from (6) that the problem must be solved in terms of the complex eigenvalue $p = d + ik$, where "d" is a damping parameter, while the aerodynamic matrices are available only for the harmonic motion and, consequently, the solutions of (6) are strictly valid only for

this type of undamped motion; nevertheless, eqn (6) is supposed to be valid also for relatively small values of "d".

Eqn. (6) is solved by an iterative procedure according to the scheme in fig. 2, showing that, for assigned values of ρ_∞ and M, the procedure of iteration is carried out for an initial speed and, subsequently, for a set of preselected speeds.

The procedure starts from suitable initial trials for p (which are indicated as

$$p_1 = d_1 + ik_1 \text{ and } p_2 = d_2 + ik_2 \text{ in fig. 2)}$$

and determine the iterated value $p_c = d_c +$

$+ ik_c$ (by means of various techniques

(e.g. /4/)) for which a prefixed degree of convergence is obtained; some kind of interpolation laws are requested to compute $[A(k_i, M_j)]$ because these matrices must be assessed at any step of the iteration.

In the "p-k method", the above mentioned disadvantages a) and b) disappear; in particular, the modification shown in the lower part of the fig. 2 to relate the input quantities by means, e.g., of the ISA, can be easily introduced into any computer program where the p-k method is implemented.

As for the previously mentioned item c), it is easy to realize that in the "p-k method" any single complex eigenvalue can be univocally associated to the relevant aeroelastic mode; the correspondent shape of the mode can be assessed successively, by making use of the general equation (6).

In order to obtain this information as a direct result of the computation procedure (avoiding also possible numerical problems relevant to the elimination of an equation in the system (6)) and, moreover, to maintain the possibilities of the "p-k method" regarding the items a) and b) mentioned above, the following solution method was adopted by the present authors.

The unknown quantities of the problem are the "n" components of the vector {q} and the complex eigenvalue p; the equations available are "n" in (4) and another one is the normalization equation; so the system to be solved is

$$(7) \begin{cases} [F] \{q\} = 0 \\ z = \frac{1}{2} \{q\}^T \{q\} - 1 = 0 \end{cases}$$

where $[F]$ is defined in (4.a), or, being the

vector {q} complex,

$$(7.a) \begin{cases} (\text{Re}[F] + i \text{Im}[F]) (\text{Re}\{q\} + \\ + i \text{Im}\{q\}) = 0 \\ \text{Re}(z) + i \text{Im}(z) = 0 \end{cases}$$

that is,

$$(7.b) \begin{cases} \text{Re}[F] \text{Re}\{q\} - \text{Im}[F] \text{Im}\{q\} = 0 \\ \text{Im}[F] \text{Re}\{q\} + \text{Re}[F] \text{Im}\{q\} = 0 \\ \text{Re}(z) = 0 \\ \text{Im}(z) = 0 \end{cases}$$

The method of solution of the system 7.a) is the classical Newton-Raphson method, the main features of which are briefly summarized in the rest of this paragraph and for more other details, reference can be made to /1/.

Let {X} indicate, for brevity sake, the unknown vector; let {r}=0 be the set of the n + 1 equations depending on {X} and, finally, let {X₀} be a reference condition; by the linear Taylor expansion from the condition {X₀} we get

$$\{r(\{X_0\})\} + [J_0] (\{X\} - \{X_0\}) = 0,$$

or

$$8) [J_0] \{\Delta X\} = \{r_0\},$$

where $\{\Delta X\} = \{X_0 - X\}$, $[J_0]$ is the

Jacobian matrix calculated in {X₀} and

$$\{r_0\} = \{r(\{X_0\})\}.$$

In the expanded form, (8) is equivalent to

$$8.a) \begin{bmatrix} \text{Re} [F] & -\text{Im} [F] & \text{Re}(v) & -\text{Im} \{v\} + \text{Re} \{w\} \\ \text{Im} [F] & \text{Re} [F] & \text{Im} \{v\} & \text{Re} \{v\} + \text{Im} \{w\} \\ \text{Re} \{q\}^T & -\text{Im} \{q\}^T & 0 & 0 \\ \text{Im} \{q\}^T & \text{Re} \{q\}^T & 0 & 0 \end{bmatrix} \begin{bmatrix} \text{Re} \{\Delta q\} \\ \text{Im} \{\Delta q\} \\ \text{Re} (\Delta p) \\ \text{Im} (\Delta p) \end{bmatrix} = \begin{bmatrix} \text{Re} \{z_0\} \\ \text{Im} \{z_0\} \\ \text{Re} (z_0) \\ \text{Im} (z_0) \end{bmatrix}$$

where

$$8.c) \{v\} = [2 \cdot [M] p + [C]] \{q\}$$

$$8.d) \{w\} = \left[-\rho_\infty \frac{V}{2} c \frac{\partial [A]}{\partial k} \right] \{q\};$$

Now, starting from the reference condition $\{X_0\}$ (that is, a certain natural mode, $\{q_0\}$ and the relevant natural eigenvalue, $p_0 = i \omega_0$, relevant to harmonic motion), the incremental vector $\{\Delta X\}$ (or that in the l.h.s. in (8.a)) is obtained by means of an

iterative procedure until a fixed convergence level is obtained; the terms of the matrix $[J_0]$ are relevant to an initial

flight speed, V_0 , (which is constant during the iterations); the previous step is repeated at $V_1 = V_0 + \Delta V$ and, subsequently, at $V_n = V_{n-1} + \Delta V$ so as to cover a pre-fixed range of significant flight speeds.

When convergence is not obtained after a maximum number of iterations at the speed $V_{i+1} = V_i + \Delta V$, the procedure is repeated at a new speed $V'_{i+1} = V_i + \alpha \Delta V$, $\alpha < 1$, and the opposite is valid when the convergence occurs too quickly; for other features of the method, reference may be made to the flow chart in fig. 3.

III. The unsteady Aerodynamic panel method

Let us consider the aerodynamic field produced by a body, which, apart from small displacements, is in translation with a constant speed $-U$ with reference to still air (assumed to be in uniform conditions).

The acoustic approximation of the air motion equations, referred to a system in translation with the same speed, $-U$, of the body is

$$9) \quad \Delta \phi = M^2 (D/Dt)^2 \phi$$

where Δ indicates the Laplace operator in the $(x_1, x_2, x_3) \equiv \underline{x}$ spatial coordinates of this reference system, ϕ is the velocity potential, $D/Dt = \partial/\partial t + \partial/\partial x_1$ with the x_1 axis fixed so that the angle between

this axis and the \underline{U} vector is very small.

All the quantities involved in (9) are non dimensional with reference to $|\underline{U}|$ and to an arbitrary length.

Note that the effects of the Mach number ($M > 0$) in (9) are linearly approximated by means of the small perturbation theory.

Let $\underline{x} = \underline{X}$ be the initial position of any material point of the body surface and $D\underline{x}$, which is assumed to be very small, the displacements of the same point; $D\underline{x}$ is taken as the contribution of the rigid and/or elastic displacements and we suppose it can be expressed by N generalized coordinates q_j so that

$$10) \quad D \underline{x} = \sum_{j=1}^N A_j(\underline{x}) q_j(t)$$

The wake is a discontinuity surface S_w embedded in the irrotational field and originating from the trailing edge so that the Kutta-Joukowski condition is satisfied; the positive and negative faces of the wake are indicated, respectively, by S_{w+} and S_{w-} .

The aerodynamic field is external to the surface $S' = S_b' + S_{w+}' + S_{w-}'$ where S_b' is the body surface; the surface S' is

approximated by means of a polyhedron whose quadrilateral faces (panels) are portions of hyperbolic paraboloids (or, in particular, of planes) with straight sides.

The parametric equation of a panel is

$$11) \quad \underline{x} + D \underline{x} = \underline{p}_0' + \xi \underline{p}_1' + \eta \underline{p}_2' + \xi \eta \underline{p}_3'$$

each pair of parameters ξ, η , with $|\xi| \leq 1, |\eta| \leq 1$, specifies a material point of the panel.

Let $\underline{x} = \underline{x}_s$ be the initial position of the s^{th} of the four corners of a panel, numbered from 1 to 4 consecutively, and $D \underline{x}_s$ be the corresponding displacement; putting, for $r = 0, 1, 2, 3$,

$$12) \quad \underline{p}_r = \sum_{s=1}^4 L_{r+1,s} \underline{x}_s$$

$$12.a) \quad \underline{p}_r = \sum_{s=1}^4 L_{r+1,s} D \underline{x}_s$$

where $L_{r+1,s}$ is the element on the $(r+1)$ th row and s -th column of the matrix

$$13) \quad \frac{1}{4} \begin{bmatrix} 1 & 1 & 1 & 1 \\ 1 & 1 & -1 & -1 \\ 1 & -1 & -1 & 1 \\ 1 & -1 & 1 & -1 \end{bmatrix}$$

we get

$$14) \quad \underline{p}_r' = \underline{p}_r + \underline{p}_r'$$

Now, the condition of tangency for the velocity of the air relevant to the body is

$$15) \quad \underline{n}' \cdot \nabla \phi = \underline{n}' \cdot \left(\frac{\partial}{\partial t} (D \underline{x}) - \underline{u} \right)$$

where ∇ indicates the gradient operator in the (x_1, x_2, x_3) coordinates, \underline{n}' is

the normal unit vector for a panel in a deformed condition, oriented towards the air; \underline{u} is the unit vector of the asymptotic speed \underline{U} ; the fluid speed \underline{v} is given by

$$16) \quad \underline{v} = \underline{u} + \nabla \phi.$$

A considerable simplification of the problem is obtained by supposing that (15) can be formulated with reference not to the real one but to the fixed body configuration, S_b^0 , relevant to $D \underline{x} \equiv 0$

This simplification is obtained by imposing the following condition (15/), giving the invariance of the flux of the vector $\nabla \phi$:

$$17) \quad \underline{n}' \cdot \nabla \phi \mid (\underline{p}_1' + \eta \underline{p}_3') \times (\underline{p}_2' + \xi \underline{p}_3') \mid d \xi d \eta = \underline{n} \cdot \nabla \phi \mid (\underline{p}_1^0 + \eta \underline{p}_3^0) \times (\underline{p}_2^0 + \xi \underline{p}_3^0) \mid d \xi d \eta$$

where the unit vector \underline{n} corresponds to \underline{n}' for S_b^0 ; in particular, in the panel centroid ($\xi = \eta = 0$) (17) becomes

$$17.a) \quad \underline{n} \cdot \nabla \phi = \left| \underline{p}_1' \times \underline{p}_2' \right| / \left| \underline{p}_1^0 \times \underline{p}_2^0 \right| \mid \underline{n}' \cdot \nabla \phi.$$

Now we can put

$$18) \quad \underline{n}' = \frac{|\underline{P}_1' \times \underline{P}_2'|}{|\underline{P}_1 \times \underline{P}_2|} = \underline{n} + \underline{Dn}$$

where \underline{Dn} is very small; from (14) we obtain

$$19) \quad \underline{Dn} = (\underline{P}_1 \times \underline{P}_2 + \underline{P}_1' \times \underline{P}_2') / |\underline{P}_1 \times \underline{P}_2|$$

when the vector product $\underline{P}_1 \times \underline{P}_2$ is disregarded.

From (10) and (12.a) we obtain

$$20) \quad \underline{p}_r = \sum_{j=1}^N \underline{p}_{rj} q_j$$

where:

$$20.a) \quad \underline{p}_{rj} = \sum_{s=1}^4 L_{r+1,s} A_j(x_s).$$

The velocity of a panel centroid is given by

$$21) \quad \underline{v}_b = \sum_{j=1}^N \underline{p}_{oj} \frac{dq_j}{dt};$$

so, from eqs (15), (17.a), (18) we have

$$22) \quad \underline{n} \cdot \nabla \phi = (\underline{n} + \underline{Dn}) \cdot (\underline{v}_b - \underline{u}) = -\underline{n} \cdot$$

$$\underline{u} + \sum_{j=1}^N (\underline{n} \cdot \underline{p}_{oj}) \frac{dq_j}{dt} - \underline{Dn}_j \cdot \underline{u} q_j$$

where

$$22.a) \quad \underline{Dn}_j = (\underline{P}_1 \times \underline{P}_2 + \underline{P}_{1j} \times \underline{P}_{2j}) / |\underline{P}_1 \times \underline{P}_2|.$$

As for the wake, the following conditions must be satisfied across the same:
- equality of the normal component of velocity

$$23) \quad \underline{v}^+ \cdot \underline{n}' = \underline{v}^- \cdot \underline{n}'$$

- equality of the pressure coefficient across

the wake

$$23.a) \quad C_p^+ = C_p^-$$

where "+" and "-" are relevant to the upper (S_w^+) and lower (S_w^-) faces of the wake, respectively.

In one point of the wake, from the Bernoulli equation and (23.a), we have

$$24) \quad \left(\frac{\partial}{\partial t} + \underline{v}_a \cdot \nabla \right) (\phi^+ - \phi^-) = 0$$

where \underline{v}_a indicates the average speed of the wake:

$$24.a) \quad \underline{v}_a = (\underline{v}^+ + \underline{v}^-) / 2.$$

In order to avoid an iterative computation of the wake shape (\underline{n}' in (23) depending on the actual configuration), as is well known, the following simplification can be applied:

$\underline{v}_a = \underline{e}_1 =$ unit vector of the x_1 axis.

In other words, the direction of the trailing vorticity does not vary with time and is very close to that of the asymptotic speed U and, therefore, the wake is substituted by a fixed surface, S_w^0 , made of straight lines originating along the trailing edge in the reference configuration ($Dx \equiv 0$) and going downstream to infinite.

With reference to fig. 4, boundary conditions on the substitutive wake are

$$25) \quad (\underline{v}^+ - \underline{v}^-) \cdot \underline{n} = 0$$

$$25.a) \quad (\phi^+ - \phi^-)_{Q,t} = (\phi^+ - \phi^-)_{(Q_{TE,t} - Q_{TE}^-)}$$

Taking into account the effects of compressibility, we now consider a new set of coordinates (x, y, z) by putting

$$26) \quad (x, y, z) = (x_1/B, x_2, x_3)$$

where $B = (1-M^2)^{\frac{1}{2}}$

We denote with N the unit vector in x, y, z space corresponding to n and with $\partial/\partial N$ the directional derivative in the direction of N ; we have

$$27) \quad \frac{\partial \phi}{\partial N} = (1-M^2 n_1^2)^{\frac{1}{2}} n \cdot \nabla \phi - \left(\frac{1-n_1^2}{1-M^2 n_1^2} \right)^{\frac{1}{2}}$$

$$M^2 n_1^2 t \cdot \nabla \phi$$

where: $n_1 = n \cdot e_1$ and $t = (e_1 - n_1 n) / |e_1 - n_1 n|$.

In the small perturbation theory for the compressibility effect we can disregard the second term in the r.h.s. of (27); we may also put

$$28) \quad 1-M^2 n_1^2 \approx 1;$$

so, eqn (27) becomes, simply:

$$29) \quad \partial \phi / \partial N = n \cdot \nabla \phi.$$

For the velocity potential in $P_0 \equiv (x_0, y_0, z_0)$ relevant to $t = t_0$ in the (x, y, z) space, we get by means of the generalized Kirchhoff formula (5/, /6/),

$$30) \quad 4 \pi E(P_0) \phi(P_0, t_0) = - \int_S n \cdot$$

$$\cdot \nabla \phi|_{t_0} \frac{dS(P)}{R} + \int_S \phi|_{t_0} \frac{\partial(1/R)}{\partial N} dS(P) -$$

$$- \int_S \frac{\partial \phi}{\partial t} |_{t_0} \frac{1}{R} \frac{\partial T}{\partial N} dS(P),$$

where : S is the closed surface in the (x, y, z) space corresponding to

$$S^0 = S_b^0 + S_{w+}^0 + S_{w-}^0 ;$$

$R = \overline{PP_0}$ is the distance between the points P and P_0 ;

$$t' = t_0 - M [M(x - x_0) + R] / B \equiv t_0 -$$

$$- \theta(P_0, P);$$

$$T = M [M(x_0 - x) + R] / B;$$

$E(P_0) = 0, 1, \frac{1}{2}$ according to whether point P_0 is external, internal or on the boundary, S , of the field; for the second integral in the r.h.s. of (30), the Cauchy principal value must be considered; the total surface S is composed of the surfaces S_b, S_{w+}, S_{w-} which correspond to $S_b^0, S_{w+}^0, S_{w-}^0$ in the reference configuration.

When P_0 is positioned on the body surface S_b , eqn (30) becomes the equation

which solves the problem.

An approximate numerical solution of (30) is obtained by taking the following steps:

- i) substituting the body surface S with a polyhedron made of quadrilateral panels, S_K , as indicated above;
- ii) for each panel S_K , the values of $n \cdot \nabla \phi|_{t_0}, \phi|_{t_0}$ and $\partial \phi / \partial t|_{t_0}$ are assumed to be constant and assessed in the panel centroid.

Now, eqn (30) is approximated by a system of algebraical equations, where the influence coefficients are

$$B_K(P_0) = - \frac{1}{2\pi} \int_{S_K} \frac{1}{R} dS(P)$$

$$31) \quad C_K(P_0) = - \frac{1}{2\pi} \int_{S_K} \frac{1}{R^2} \frac{\partial R}{\partial N} dS(P)$$

$$D_K(P_0) = - \frac{1}{2\pi} \int_{S_K} \frac{\partial T}{\partial N} \frac{1}{R} dS(P)$$

The following (/5/) is an approximate evaluation of $D_K(P_0)$:

$$D_K(P_0) = -M^2 B_K(P_0) N(P_0) \cdot e_{-1}/B +$$

$$+ M \overline{P_0 P_K} C_K(P_0)/B \text{ where } P_K \text{ is the centroid of the } S_k \text{ panel; the coefficients } C_K(P_0) \text{ and (for flat panels) } B_K(P_0) \text{ can}$$

be evaluated in a closed form (/7/,/8/).

We shall now consider the unsteady part of the aerodynamic field and we suppose the motion to be harmonic; by putting

$$32) \quad q_j = \tilde{q}_j \exp(i \omega t) \quad (\omega \text{ indicates the circular frequency})$$

$$33) \quad \phi = \tilde{\phi}_j q_j$$

$$34) \quad \tilde{\psi}_j = i \omega \tilde{n} \cdot \tilde{p}_{0j} - \tilde{u} \cdot \tilde{Dn}_j,$$

we have

$$35) \quad \tilde{n} \cdot \nabla \tilde{\phi}_j = \tilde{\psi}_j$$

and the problem can be reduced to the solution of the following algebraical set of equations:

$$36) \quad \langle A_{H,K} \rangle \langle \tilde{\phi}_j(P_K) \rangle =$$

$$= \langle B_{H,K} \rangle \langle \tilde{\psi}_j(P_K) \rangle.$$

This is a linear system where $\tilde{\phi}_j(P_K)$

are the unknown quantities; each non-homogeneous term is given by a linear combination of the values $\tilde{\psi}_j(P_K)$ assumed in the centroids P_K ; the symbols in (36) indicate the following quantities:

$$36.a) \quad B_{H,K} = B_K(P_H) E_{H,K} \text{ where}$$

$$36.b) \quad E_{HK} = \exp(-i \omega \Theta(P_H, P_K))$$

$$36.c) \quad A_{H,K} = W_{H,K} + \delta_{H,K} - (C_K(P_H) +$$

$$+ i \omega D_K(P_H)) E_{H,K}$$

where $\delta_{H,K}$ is the Kronecker delta and

$$36.d) \quad W_{H,K} = \sum_L \delta_{K,I(L)} [C_L(P_H) +$$

$$+ i \omega D_L(P_H)] E_{H,L} F_{L,I(L)}$$

where

$$36.e) \quad F_{L,I} = \exp(-i \omega B(x(P_L) - x(P_I)))$$

The index L is relevant to a panel in the wake; the index I(L) (fig.5) is relevant to the body panel at the trailing edge in the same longitudinal row of panels and the same face (upper or lower) of the panel "L"; H and K are the indexes of the body panels.

Any longitudinal row of panels in the wake is truncated at a downstream distance of about 5 mean chords from the trailing edge.

Now, as is well known, the Bernoulli theorem in isentropic unsteady conditions is

$$37) \quad \frac{\partial \phi}{\partial t} + \tilde{u} \cdot \nabla \phi + \frac{1}{2} \nabla \phi \cdot \nabla \phi + h = h_\infty$$

where h is the enthalpy (per unit mass divided by $|U|^2$) and h_∞ is the enthalpy relevant to undisturbed fluid.

Let $\phi = \phi_0$ be the solution in the reference condition ($Dx \equiv 0$); putting

$\phi = \phi_o + \phi_d$, we suppose that $\nabla\phi_d$ is so small that

$$37.a) \quad |\nabla\phi_o|^2 + 2 \nabla\phi_o \cdot \nabla\phi_d + |\nabla\phi_d|^2 \approx |\nabla\phi_o|^2 + 2 \nabla\phi_o \cdot \nabla\phi_d$$

and

$$37.b) \quad \underline{u} \cdot \nabla\phi \approx \underline{u} \cdot \nabla\phi_o + \frac{\partial}{\partial x_1} \phi_d$$

Therefore, by means of (37), (37.a) and (37.b), we obtain the following linear dependance of the enthalpy on ϕ_d :

$$38) \quad h - h_o = - \left(\frac{\partial\phi_d}{\partial t} + \frac{\partial\phi_d}{\partial x_1} + \nabla\phi_o \cdot \nabla\phi_d \right)$$

where h_o is the local enthalpy, h , for the solution ϕ_o .

The increment of the pressure coefficient between reference and actual configurations can be calculated as

$$39) \quad DC_p = C_p - C_{p_o} = 2 \frac{\rho_o}{\rho_\infty} (h - h_o)$$

where, as is well known, the ratio between the local density relevant to $Dx=0$ and the undisturbed fluid density is expressed as follows

$$40) \quad \rho_o/\rho_\infty = \left[1 + \frac{\mu-1}{2} M^2 (1 - V_o \cdot \underline{V}_o) \right]^{1/(\mu-1)}, \text{ with } \underline{V}_o = \underline{u} + \nabla\phi_o$$

where μ indicates the ratio of specific heat coefficients.

In the case of small pressure perturbations, such as those we suppose to exist here, the following simplified expression is used

$$41) \quad DC_p = C_p - C_{p_o} \approx -2 \left(\frac{\partial\phi_d}{\partial t} + \frac{\partial\phi_d}{\partial x_1} \right)$$

$$\text{with } C_{p_o} \approx 1 - |\underline{V}_o|^2.$$

The calculation of the gradient $\nabla\phi$ permits us to determine the aerodynamic forces. We already know the scalar quantity $\nabla\phi \cdot \underline{n}$ on the panel centroids; so the derivatives $\frac{\partial\phi}{\partial \xi}$ and $\frac{\partial\phi}{\partial \eta}$ obtained by means of the finite differences method, using the ϕ values in the centroids of contiguous panels, must be evaluated; the possible situations are shown in fig. 6.

The generalized forces per unit of dynamic pressure corresponding to the displacements Dx are:

$$\sum_K (-DC_p) \underline{n}_K \cdot \underline{A}_H a_K$$

where a_K is the area of the S_K body panel in the reference configuration; DC_p , \underline{n}_K , \underline{A}_H are relevant to the centroid of the panel S_K .

Fig. 7 shows the flow chart of the computer program prepared on the basis of the aforementioned theory.

It must be noted that, by changing the frequency, a set of aerodynamic matrices is obtained at any given value of M , without repeating the calculation of the values of the coefficients B_K , C_K , D_K given by (31).

The generalized forces have been computed for the harmonic oscillations of the body because the program is used for the assessment of critical flutter conditions.

In order to check the reliability of the aerodynamic program, typical test cases were considered; some of the results obtained are to be found in the following figures: figs. 8 show a comparison between the results of the computer program and those in /9/, relevant to a wing in bending vibration; figs. 9 and 10 refer to test cases in /10/; figs. 9, in particular, concern a swept wing with a small amplitude vibrating full span aileron and figs. 10 show similar results obtained with a partial aileron.

The results obtained are in satisfactory accordance with the experimental and theoretical results, even though a relatively small number of panels was used.

Now, the description of a mode in an actual structure is generally obtained in terms of the nodal displacements of a mesh, which is designed to solve the elastodyna-

mic problem; in order to translate this mode into nodal displacements of an aerodynamic mesh, a suitable interpolation program has been set up.

The general flow-chart of this program is given in fig. 11, from which the procedure to obtain the position of any node of the aerodynamic mesh on the basis of the elastic or rigid displacements of the structural mesh, can be easily deduced.

IV. Interpolation of aerodynamic coefficients

The aerodynamic matrices $[A(k,M)]$, together with their derivatives with respect to k (as (8.d) indicates), must be known for every iteration of the flutter solution procedure adopted in the present paper, in correspondance to the values of k and M for which the iterations are carried out.

The values of k depend on the solutions ($\Delta p = \Delta d + i \Delta k$) of (8.a) relevant to all the prefixed speeds of interest

$$(V_i = V_{i-1} + \Delta V).$$

As far as M is concerned, a constant value of the Mach number is maintained in the flutter analysis at constant altitude; this is only a reference value for the computation of the aerodynamic forces.

In the variable altitude flutter analysis, a set of M (typically 0.1; 0.3; 0.5; 0.7) is planned for which the aerodynamic matrices are calculated by means of the relevant computer program, mentioned above; a range of speeds corresponds to any of these values of M relevant to the prefixed altitude range (0-11.000 m) when the already mentioned ISA is used to relate the air density to the speed of sound.

As fig. 12 shows, these ranges of speeds relevant to the values of M used do not intersect and, therefore certain new other aerodynamic matrices relevant to intermediate values of M must be provided to cover the complete range of speed, V .

In conclusion, in order to avoid having to calculate the aerodynamic matrices and their derivatives $\partial [A(k,M)] / \partial M$

by means of the relevant time consuming computer program, certain interpolation procedures, a), between the matrices

$$[A(k_i, M_j)] \text{ and } [A(k_i, M_{j+1})] \text{ and, b),}$$

$$\text{between } [A(k_i, M_j)] \text{ and } [A(k_{i+1}, M_j)]$$

must be provided.

The elements of $[A(k,M)]$ show a smooth dependence on k and M ; so, a limited number of aerodynamic computations may be carried out and, besides, simple interpolation algorithms may be used.

In the present paper, the a) interpolations are carried out by means of cubic splines and the b) interpolations may be obtained by using cubic splines or a Padè approximation.

A cubic spline function, S , is a set of piecewise cubic polynomials, defined as

$$42) \quad S(X) = \frac{X_{i+1}-X}{h} B_i + \frac{X-X_i}{h} B_{i+1} + \\ + \left(\frac{X_{i+1}-X}{h}\right)^3 (Y_i - B_i) + \left(\frac{X-X_i}{h}\right)^3 (Y_{i+1} - B_{i+1}) \quad i = 1, 2 \dots N$$

over any interval (X_i, X_{i+1}) of the range

of the variable X , where $N+1$ is the number of the equispaced abscissas of X (that is of M in the a) interpolations and of k in the b) interpolations);

$h = X_{i+1} - X_i$ are equal intervals in the range of interest of X ;

Y_i is the known value of the function $Y(X)$, corresponding to the value X_i , B_i are properly defined terms (/11/)

As for the choice of N , a compromise is necessary in order to avoid the two apposite disadvantages of, on one side, numerical instability for too great values of N (e.g. $N > 40$ must be avoided according to /11/) and, on the other hand, of a very rough approximation for small values of N .

As is well known, the Padè approximation provides an evaluation of the aerodynamic matrices $[A(p,M)]$ in presence of damping (i.e. $p = d + i\omega$, $d \neq 0$) for $M = \bar{M} = \text{constant}$, starting from their value relevant to the harmonic motion.

The Padè expression of $[A(p,\bar{M})]$ is

$$43) [A(p, \bar{M})] = [A_0(\bar{M})] + [A_1(\bar{M})] p +$$

$$+ [A_2(\bar{M})] p^2 + \sum_{j=1}^1 \frac{p}{p+r_j} [D_j(\bar{M})]$$

where $[A_0(\bar{M})], [A_1(\bar{M})], [A_2(\bar{M})], [D_j(\bar{M})]$

are real unknown matrices and r_j are real scalars, which can be either assigned "a priori" or considered as unknown.

In the present paper, as a consequence of some computations carried out by the present authors and in accordance with what other authors have done, four $[D_j]$ matrices were considered ($j=1,2,3,4$), the scalars r_j were fixed so as to avoid having a non-linear system; furthermore, in order to cover all the important aerodynamic time lag effects relevant to each of the terms $p/(p+r_j)$, these constants r_j are assigned in the range of the reduced frequencies k_j .

The unknown matrices $[A_0(\bar{M})], [A_1(\bar{M})], [A_2(\bar{M})]$ and $[D_j(\bar{M})], j=1,2,3,4,$

are assessed by means of the least square method on the basis of $m = 10$ aerodynamic

matrices $[A(p_j, \bar{M})]$, corresponding to the harmonic motion $p_j = i k_j$; so, being

$[A(p_j, \bar{M})]$ complex matrices, $2m = 20$ equations are involved.

Good results have been obtained where the constants r_1, r_2, r_3, r_4 are assigned so as to be equispaced and r_1 and r_4 are equal, respectively, to the minimum and to the maximum value of k_j .

Figs. 13, 14, 15, 16 show examples of the application of cubic splines and Padé approximation to the interpolation of some aerodynamic coefficients vs. the reduced frequency.

V. Applications

In this paragraph, two examples of application of the flutter solution computer program are described.

The first example, fig. 17, is well known to students of aeroelasticity; it is the clamped unswept wing examined in /12/, in which two artificial modes (bending and torque) are considered and the aerodynamic coefficients are assessed by the strip-theory at sea-level ($z=0$) and at the constant value $M=0$ (independently of the critical flutter speed).

These two last conditions ($z=0, M=0$) have been maintained in order to compare the results which were obtained with those reported in the above mentioned reference /12/, whereas the modes and eigenvalues were calculated once again, starting from the bending, torsional and shear stiffness curves reported in /12/, with the following results: the torsion eigenvalue was the same as that in /12/, but the bending eigenvalue was lower (11.583 instead of 12.799 rad/sec.).

The aerodynamic generalized forces were determined in relation to the different models in fig. 18, corresponding to 84,120,180 and 264 panels and to different altitudes and Mach numbers; at the reference conditions of sea-level and $M=0$, the results obtained (some of which are reported in figs. 19) show that no appreciable difference exists between 120,180 and 264 panels, so that this last model was no longer investigated since it was very time-consuming. Fig. 20 shows some of the analyses performed and the corresponding flutter speed and pulsation using different interpolation methods, different panel schematizations and different speed increments, in the same conditions of sea level and $M=0$; the analyses no. 8 and 9 in fig. 20 are relevant to the strip theory and are given in /12/.

It transpires from fig. 20 that:

- i) the results obtained do not depend on interpolation used (as fig. 21 and 22 corresponding, respectively, to cubic spline and Padé approximation confirm);
- ii) the present aerodynamic model is stable with respect to the number (N) of the panels, when $N \geq 120$;
- iii) a rough aerodynamic mesh gives rise to an unconservative prediction of the flutter speed (fig. 23)
- iv) the difference between the flutter speeds for the models 8 and 9 in fig. 20 seems to be remarkable with

respect to the stability shown by the present flutter speed prediction;

- v) the difference between the present flutter prediction and that relevant to the strip theory is quite remarkable even though the generalized mass matrices are slightly different.

The generalized aerodynamic forces corresponding to the present unswept wing depend on the Mach number according to, for example, figs. , where the results are regular in the range $M=0.5$, but considerable variations may exist between $M=0.5$ and $M=0.7$.

The second example is a free vibrating wing with a load suspended by means of a pylon; the finite element structural model, fig. , consists of beam elements and point masses.

The dynamic analysis was carried out by the MARC program providing rigid symmetric and antisymmetric modes but only the rigid and elastic symmetric modes were considered in the present flutter analysis; fig.26 shows a typical symmetric mode.

An example of aerodynamic mesh is given in fig.26 ; it is a standard mesh where panels have two parallel sides along the asymptotic stream.

The evolution of the aeroelastic modes is shown in fig.27 , which indicates that the mode becoming critical for flutter is connected to the elastic properties of the pylon.

VI. Conclusions

A procedure for the solution of flutter problems has been presented in which the aerodynamic problem has been solved by means of a tridimensional unsteady panel method. In order to calculate rapidly aerodynamic forces at intermediate Mach numbers and frequencies both cubic splines and a Padé approximation have been used as interpolation formulae.

The evolution of computation methods in aeroelasticity is connected also to the possibility of obtaining a good compromise between the need to reduce computation time and the need for an accurate prediction of aerodynamic forces.

The unsteady aerodynamic panel method presented in this paper shows a remarkable stability with respect to the refinement of the aerodynamic mesh, if a

minimum number of panels is applied; as for the present applications, the aerodynamic method was proved to be reliable and simple.

Different possible methods exist to solve the flutter equation and different versions exist of the method implemented in the present paper too (/2/); nevertheless, it is opinion of the present authors that more attention must be devoted to the solution of the unsteady aerodynamic problems in order to increase reliability and diminish time consumption.

References

- /1/ - Montegazza P., Cardani C. - "An iterative technique to compute flutter speed through the simultaneous solution of each aeroelastic mode and frequency at increasing speed". L'Aerotecnica Missili e Spazio n. 54 pp. 286-291 Oct.-Dec. 1975.
- /2/ - Cardani C., Montegazza P. - "Continuation and direct solution of the flutter equation", Computers & Structures, vol. 8, 1978, pp. 185-192.
- /3/ - Hassig H.J. - "An approximate true damping solution of the flutter equation by determinant iteration", Journal of Aircraft, vol. 8, No 11, Nov. 1971, pp.885-889.
- /4/ - Anon - "MSC Nastran, aeroelastic supplement", pp. 2.4-1, 2.4-10.
- /5/ - Morino L. - "Steady, oscillatory and unsteady subsonic and supersonic aerodynamics - production version (Soussa-P. 1.1) vol. I, Theoretical manual"- NASA CR 159130, Jan. 1980.
- /6/ - Polito L. - "Le equazioni dell'Aerodinamica subsonica e supersonica non stazionaria come generalizzazione della formula di Kirchhoff" L'Aerotecnica Missili e Spazio, vol. 62, n. 3, Sett. 1983, pp. 170-177.
- /7/ - Morino L., Chen L.T., Suci E.O. - "Steady and oscillatory subsonic and supersonic aerodynamics around complex configurations". AIAA J., vol. 13 n° 3, March 1975, pp. 368-374.

- /8/ - Lombardi G., Polito L. - "Calcolo delle azioni aerodinamiche stazionarie e non stazionarie per configurazioni ala-fusoliera in regime subsonico". Atti del VII Congresso Nazionale AIDAA Napoli, ottobre 1983, vol. I, pp. 209-222.
- /9/ - Lessing H.C., Troutman J.L., Menees G.P. - "Experimental determination of the pressure distribution on a rectangular wing oscillating in the first bending mode for Mach numbers from 0,24 to 1,30"- NASA TND-344.
- /10/ - Försching H., Triebstein H., Wagner J. - "Pressure measurements on harmonically oscillating swept wing with two control surfaces in incompressible flow". Agard CP-80-71, Part II, pp. 15-15/12.
- /11/ - Desmarais R.N., Bennet R.M. - "An automated procedure for computing flutter eigenvalues", J. of Aircraft, vol. 11, No. 2, Feb. 1974, pp. 75-80.
- /12/ - Bisplinghoff R.L., Ashley H., Halfman R.L. - "Aeroelasticity" Addison - W. Publishing, 1975.

The authors gratefully acknowledge the contribution of the students A. NALDINI and V. VACCARO, who prepared the draft of the computer program.

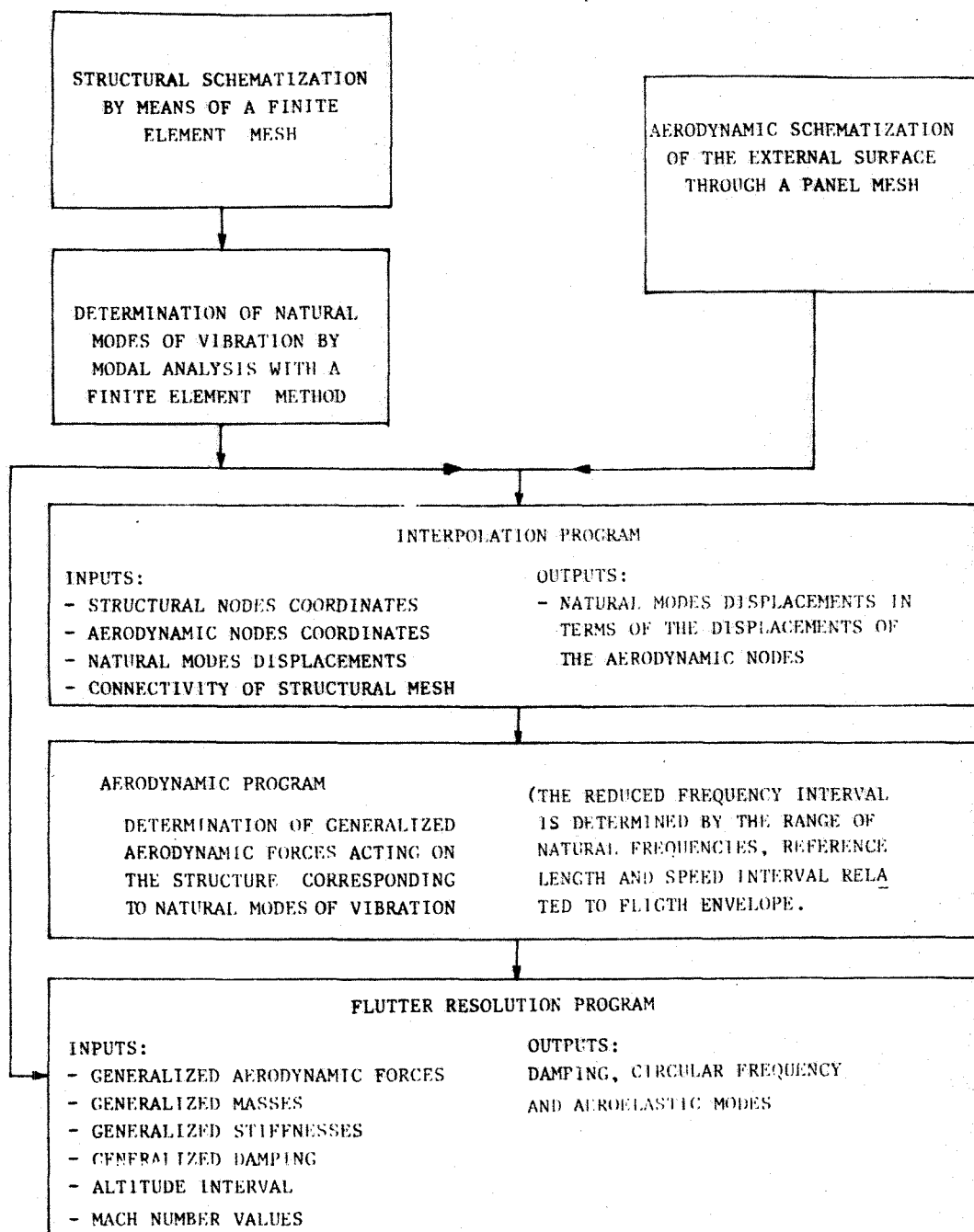


Fig.1 - Flow-chart of the general computer program.

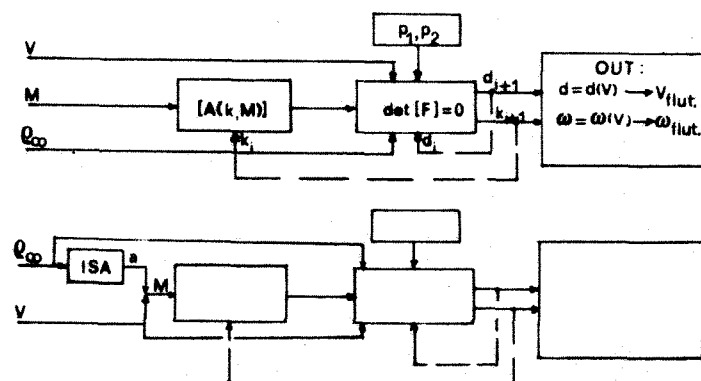


Fig.2 - p-k method flutter solution procedure.

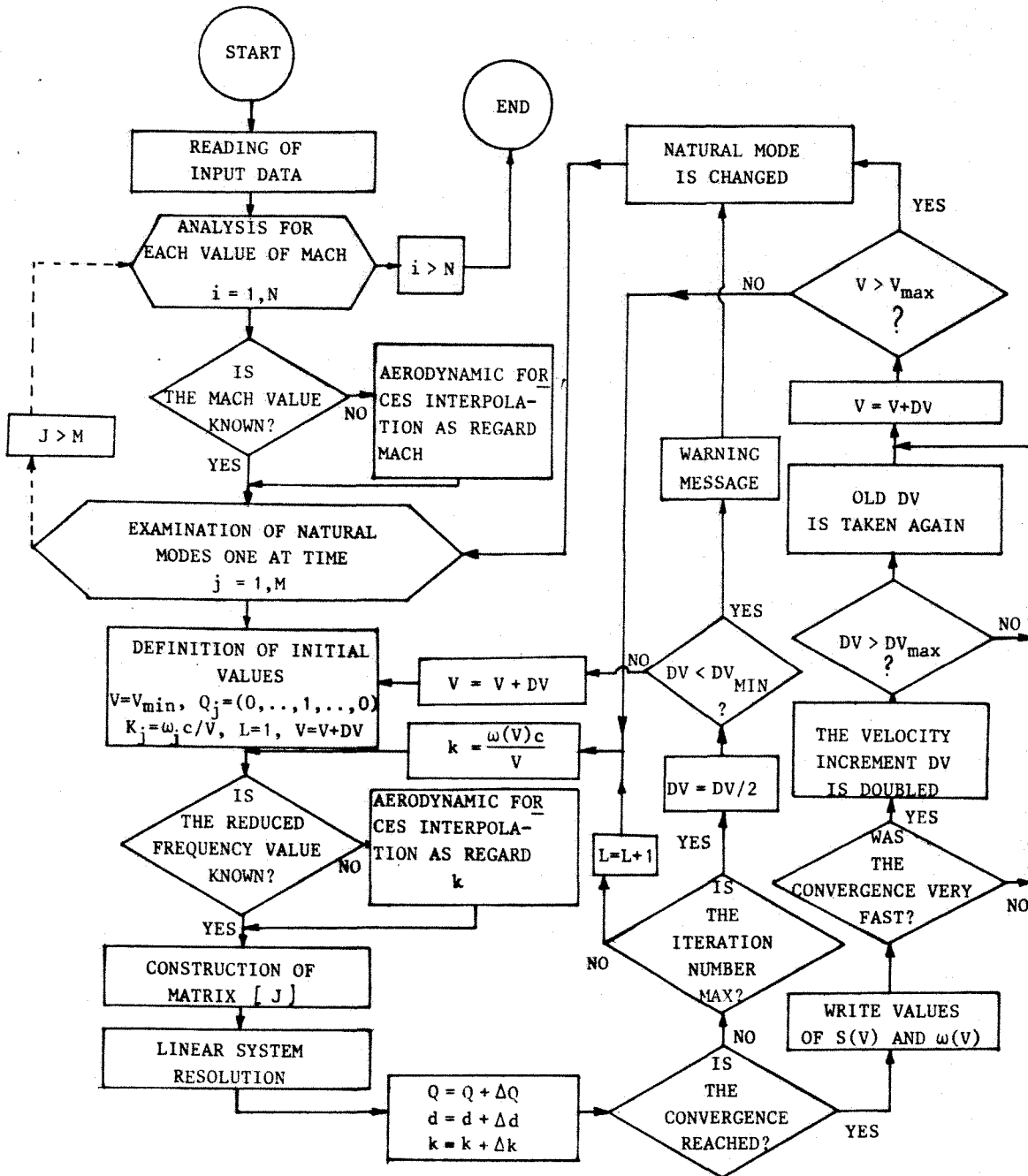


Fig.3 - Flow-chart of the present iterative flutter solution procedure.

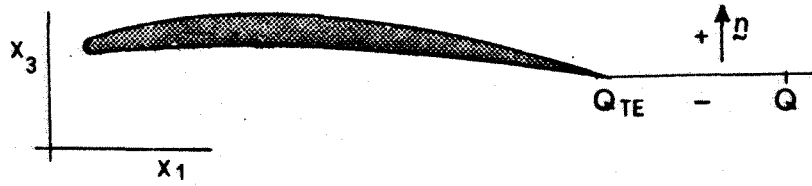


Fig. 4 - Sketch for the wake symbols

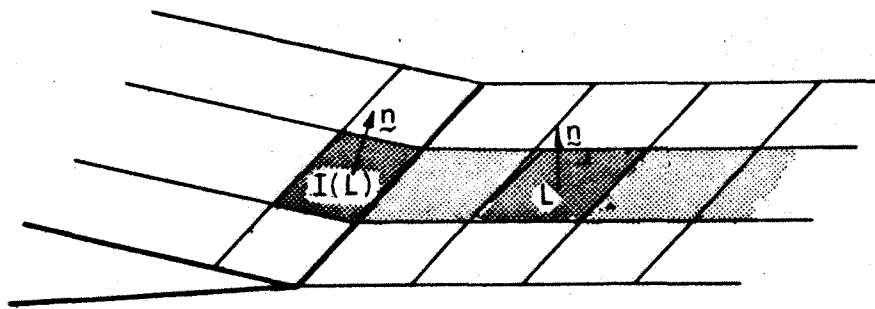


Fig. 5 - Correspondence between the trailing edge and wake panels.

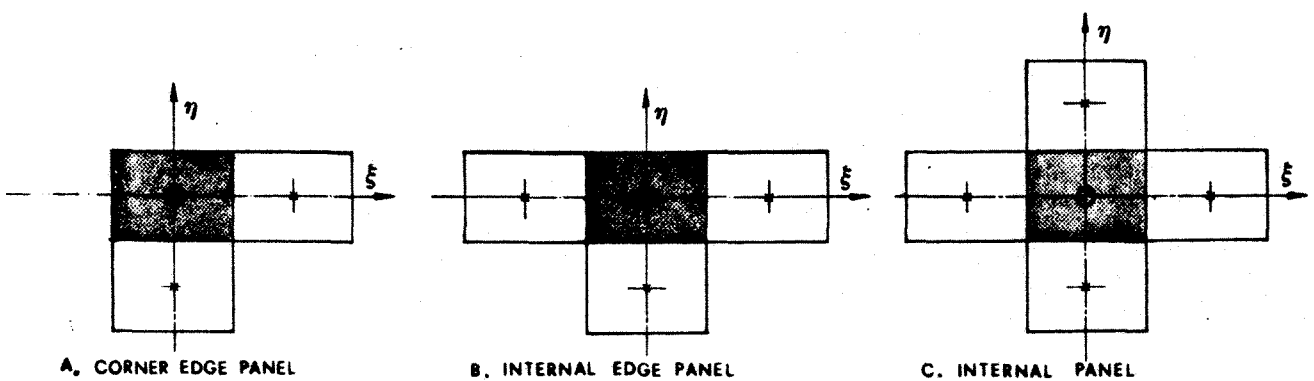


Fig. 6 - Possible panel positions on the body.

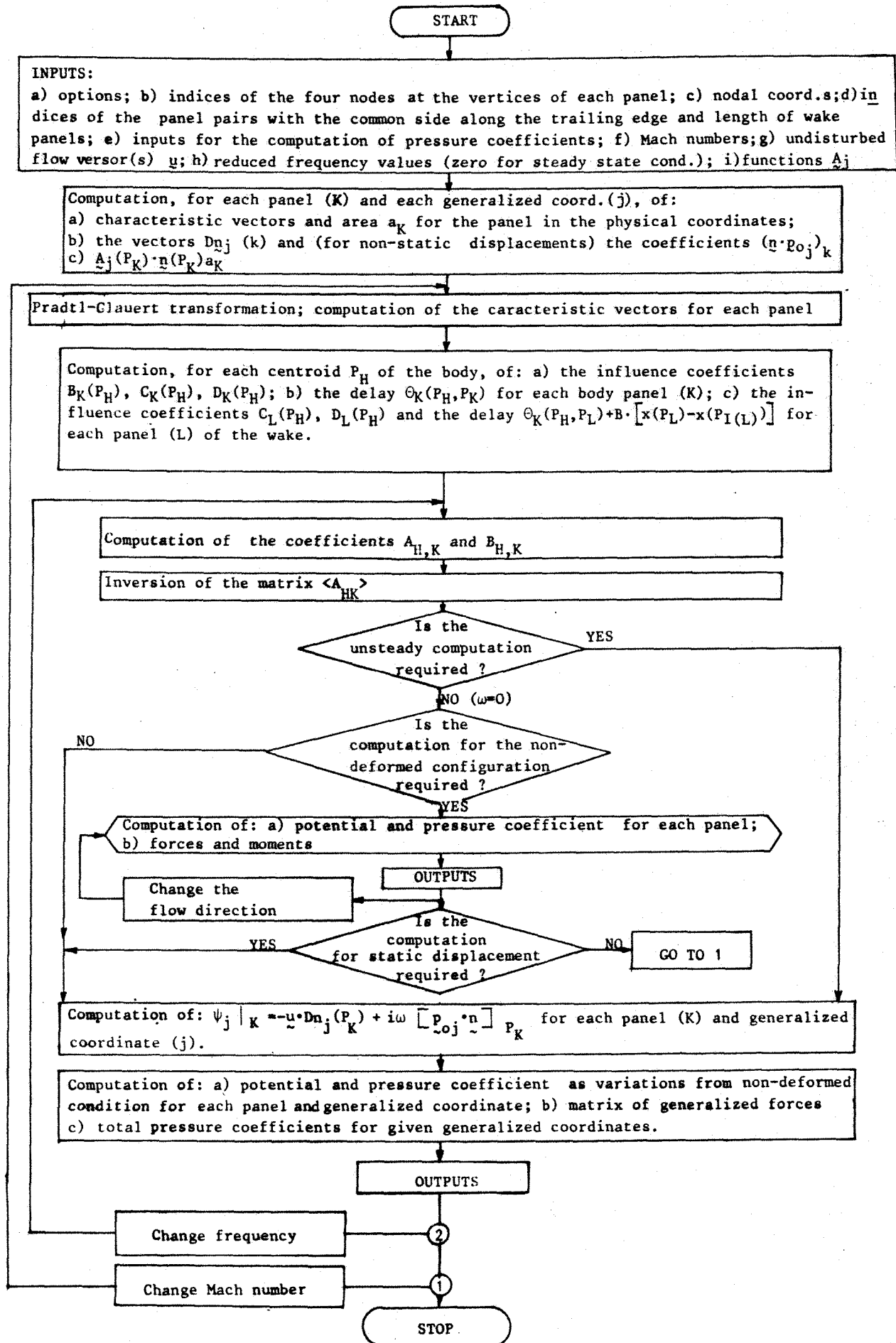
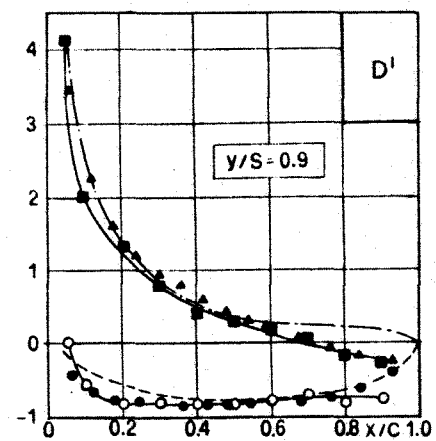
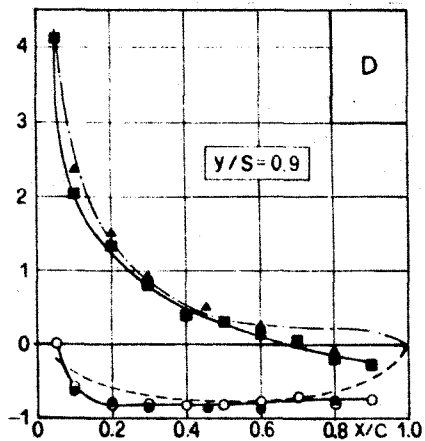
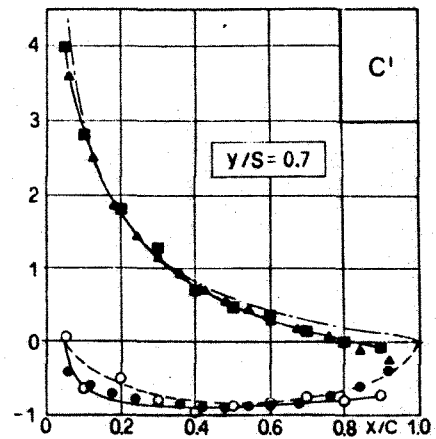
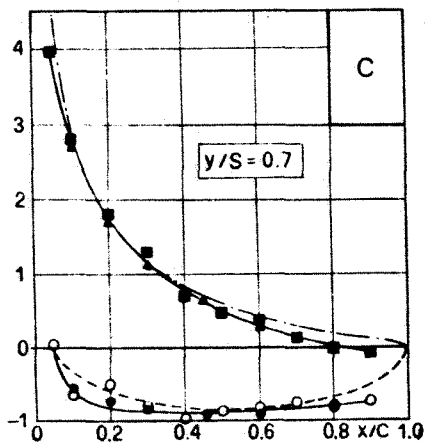
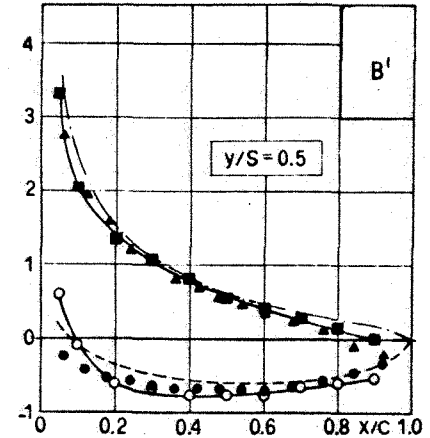
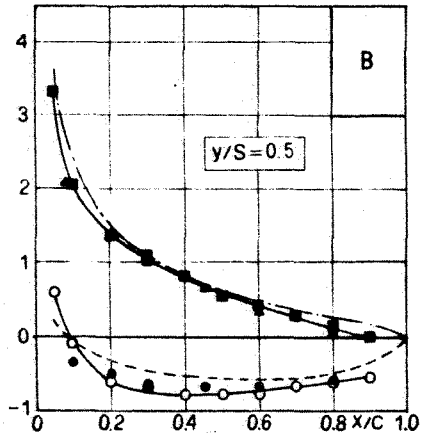
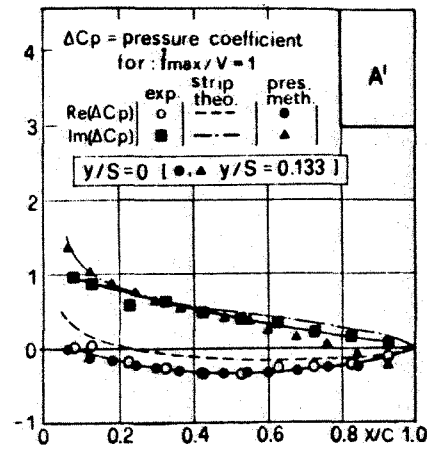
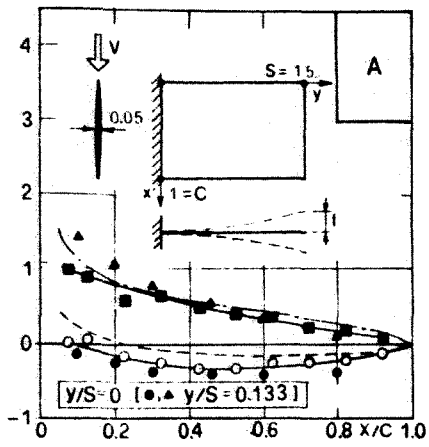


Fig.7 - Aerodynamic computer program flow-chart.



a. Body panels $5 \times (7+7)$; wake strip panels 10×0.2 c.

b. Body panels $6 \times (15+15)$; wake strip panels 30×0.13 c.

Fig.8 - Present ΔC_p and those in /9/ for bending vibrations; experiments of NASA-TND 344, $M=0.24$, $Re=2.2 \cdot 10^6$, $\omega=0.94$, angle of attack $=0^\circ$.

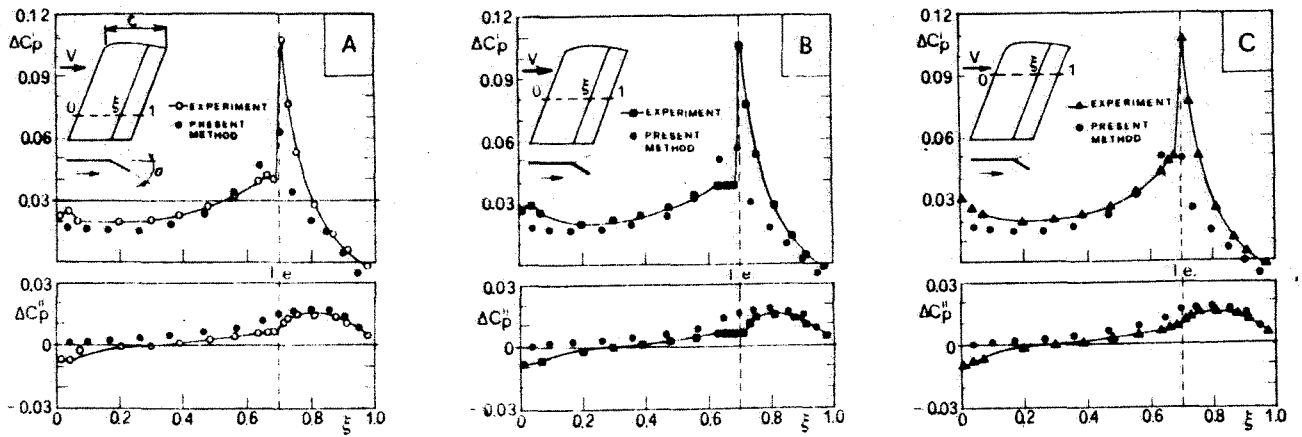


Fig. 9 - Results relevant to swept wing with a full span aileron; wing section: NACA 0012 (from AGARD CP-80/71); C_p = Pressure coefficient and $\Delta C_p' = \text{Re} \Delta C_p$, $\Delta C_p'' = \text{Im} \Delta C_p$, $M = 0$, angle of attack $= 0^\circ$, $\omega = 0.744$, $\sigma = 0.82^\circ$, body panels: $9 \times (15 \times 15)$; P_p wake strip panels: $30 \times 0.1c$

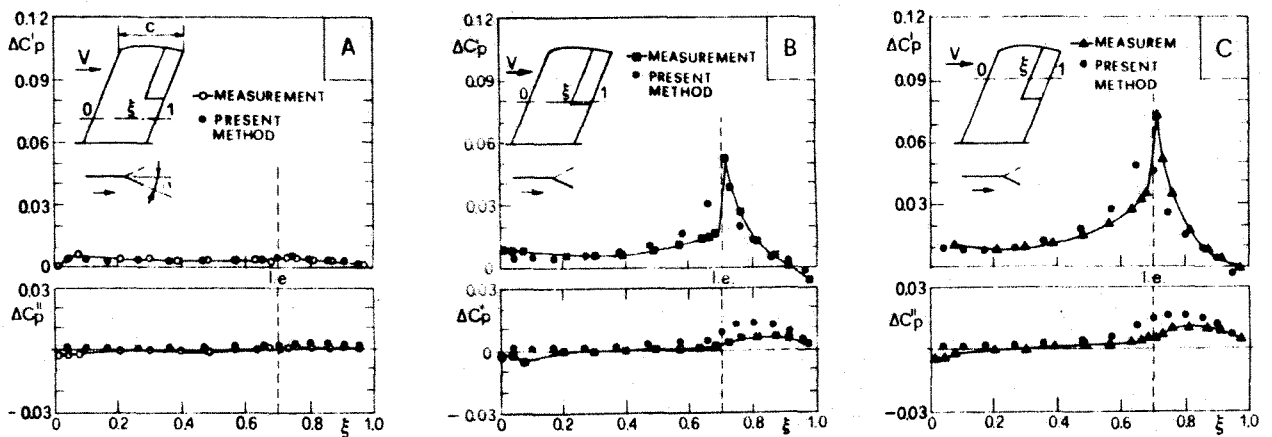


Fig. 10 - Results relevant to swept wing with a partial aileron in the same conditions as those in Fig. 9, with $\sigma = 0.66^\circ$

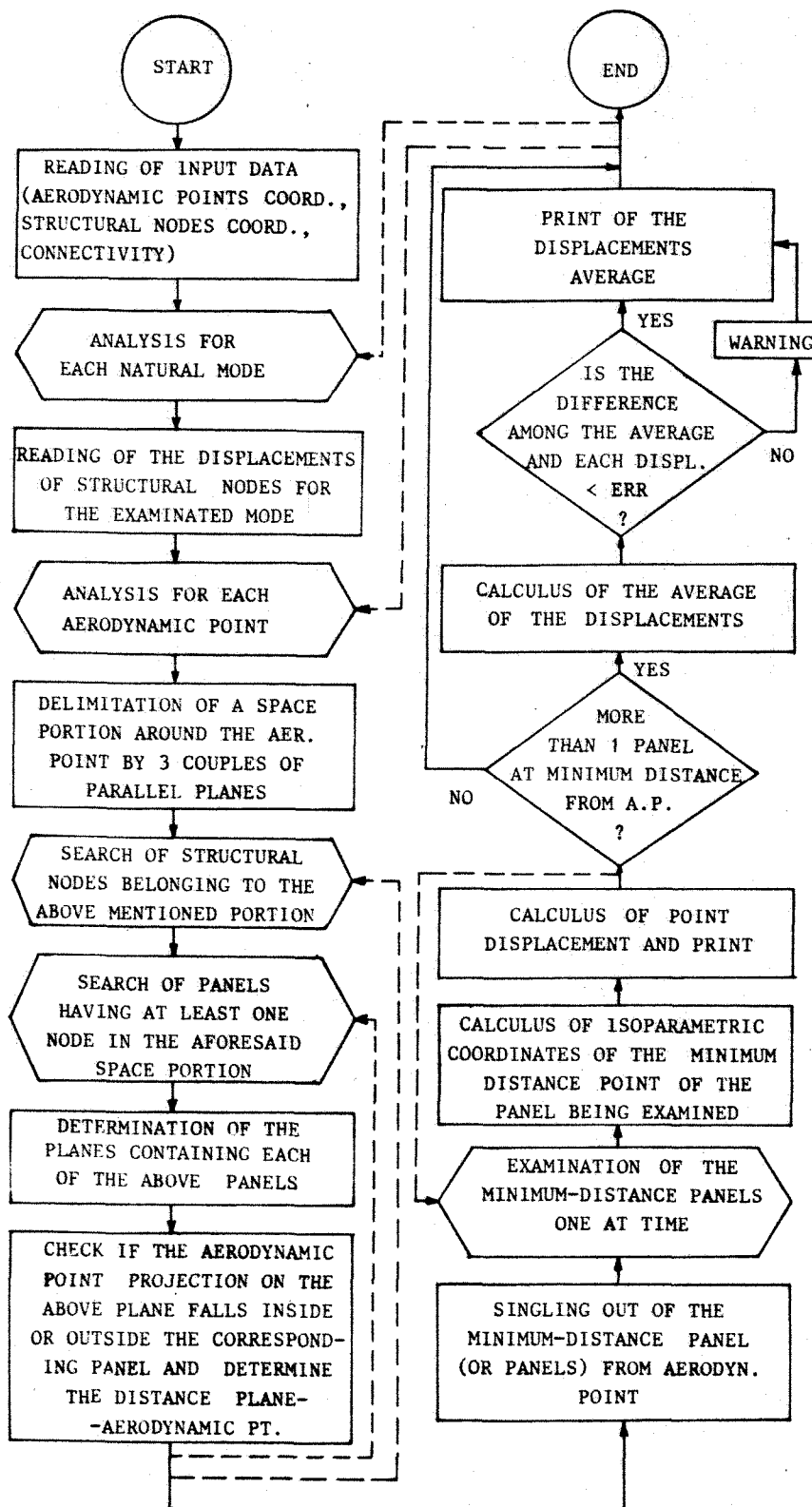


Fig. 11 - Flow-chart of the program translating a mode from the structural mesh to the aerodynamic one.

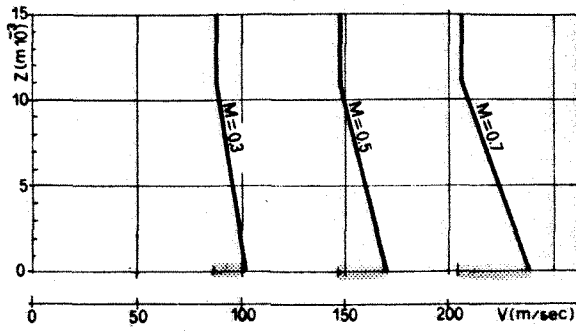


Fig.12 - Relationship between altitude and speed at constant M.

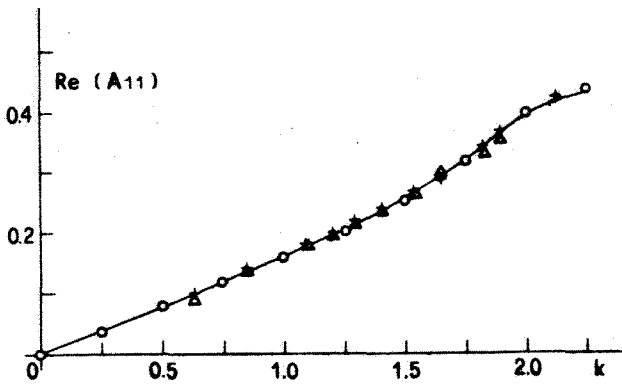


Fig.13 - Example of interpolation in terms of reduced frequency; O=values to be interpolated +=cubic spline Δ=Padé

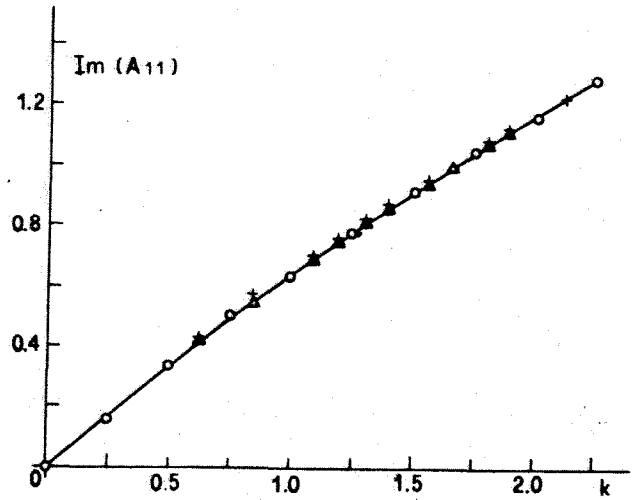


Fig.14 -

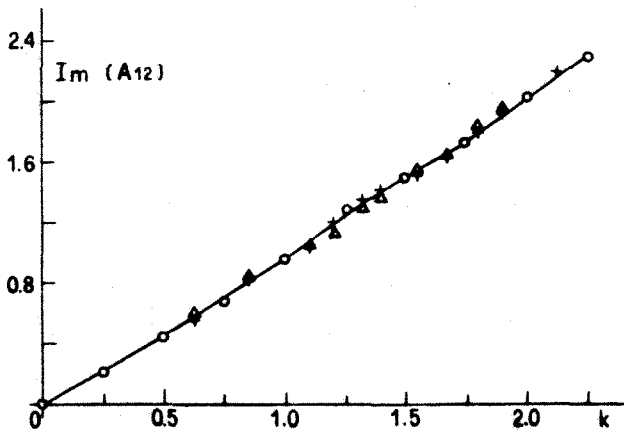


Fig.15 -

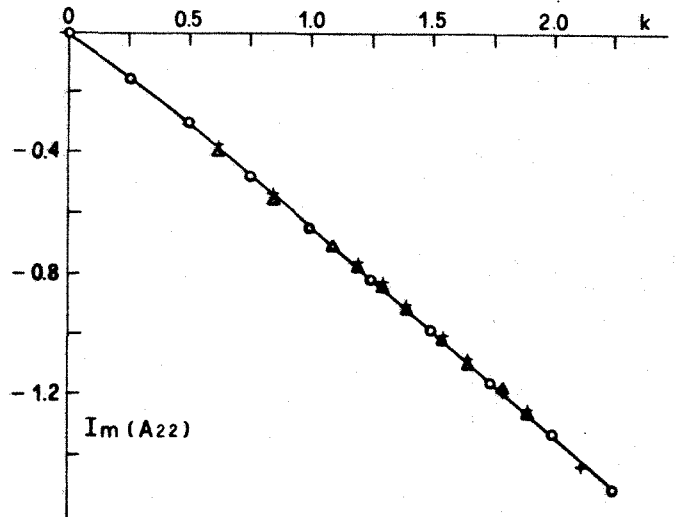


Fig.16 -

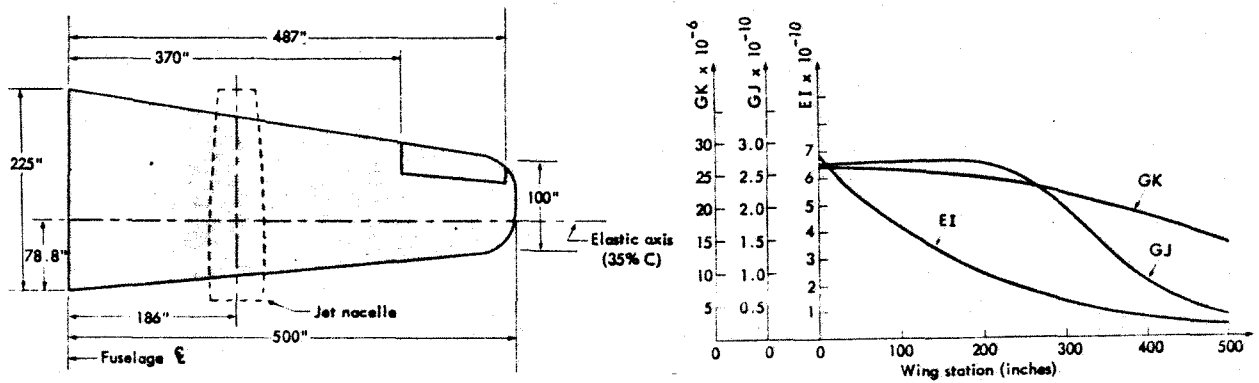


Fig.17 - Unswept wing flutter speed assessment; (from /12/).

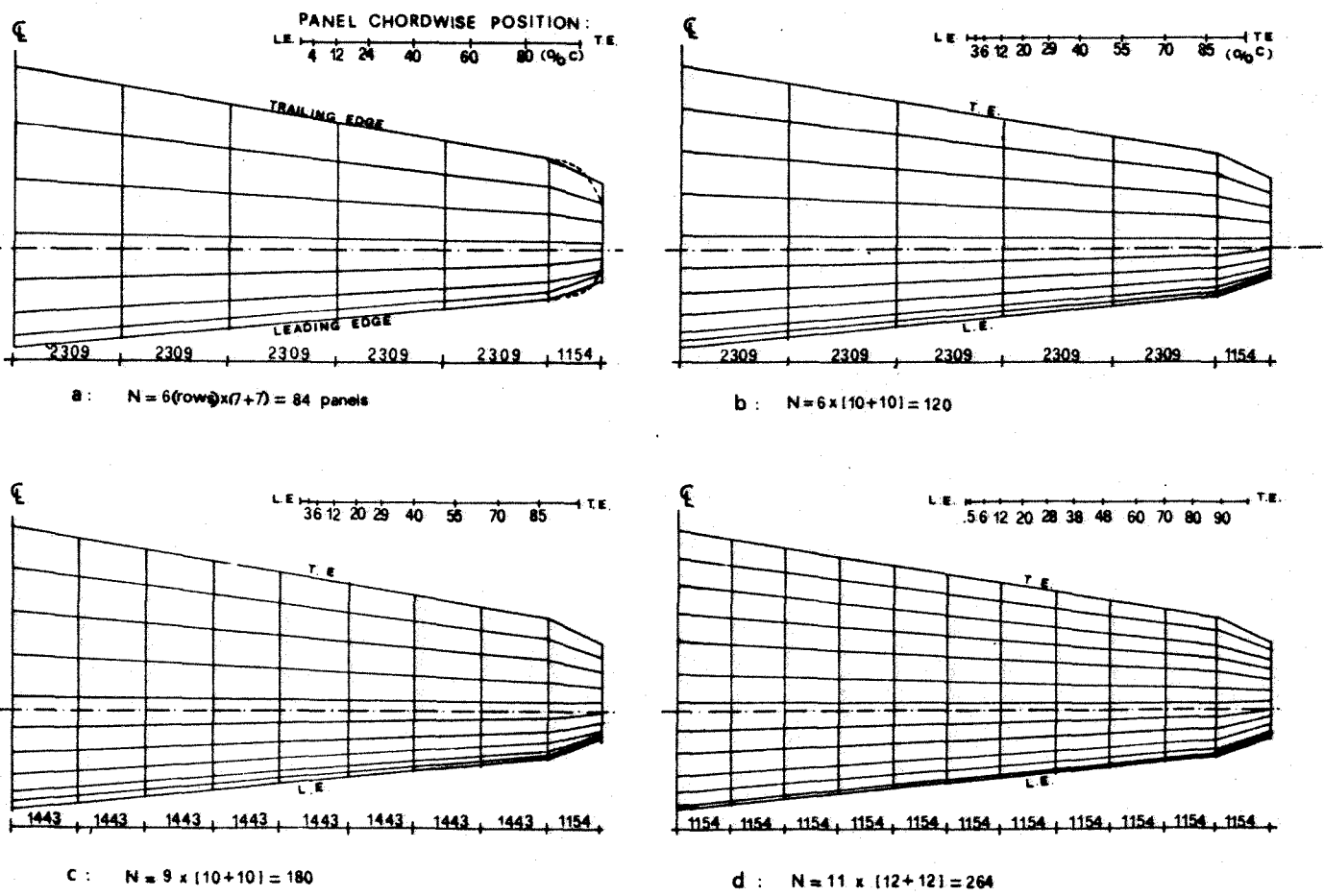


Fig.18 - The four models of aerodynamic mesh relevant to the wing in Fig. 17; wing section NACA 0012.

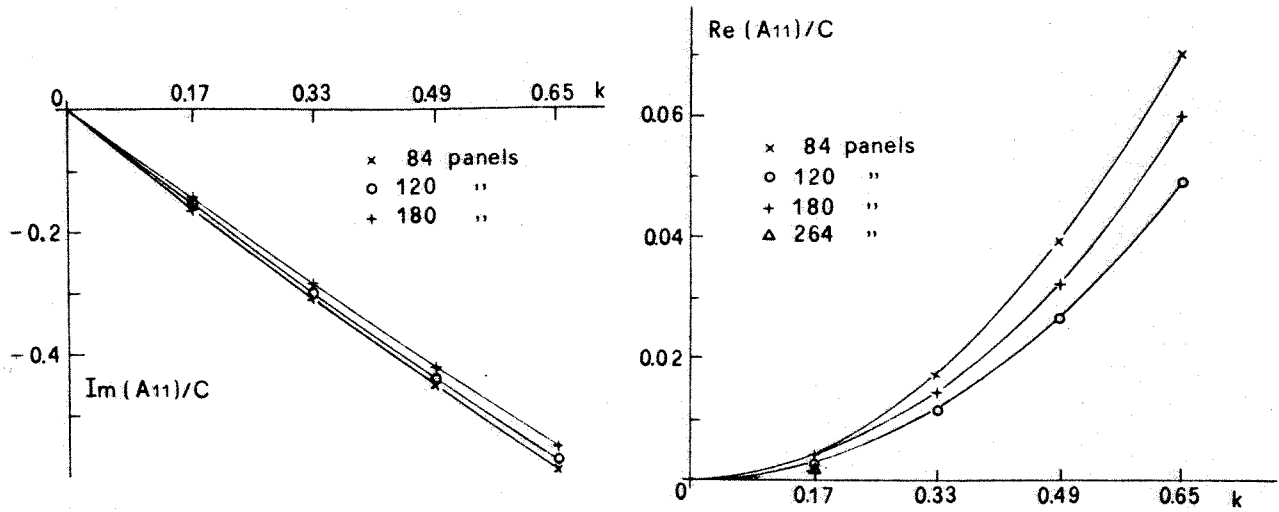


Fig.19 - Influence of the aerodynamic mesh refinement on the aerodynamic forces.

No ANALYSIS	ALTITUDE z (m)	PANELS	INTERPOLATION	ΔV (m/sec)	CRITICAL MODE No.	FLUTTER SPEED (m/sec)	ω_f (rad/sec)
1	0	84	Padè	20	2	412.01	18.517
2	0	84	Spline	20	2	411.80	18.527
3	0	120	Spline	20	2	370.26	18.882
4	0	120	Spline	5	2	371.13	18.867
5	0	120	Padè	20	2	370.27	18.879
6	0	120	Padè	5	2	371.32	18.861
7	0	180	Spline	20	2	372.97	18.747
8 ⁻	0	-	-	-	2	386.607	18.600
9 ⁻	0	-	-	-	2	426.832	17.900

- By /12/, strip theory;

- By /12/, strip theory including finite-span effects by Reissner's theory.

Fig.20 - Set of the unswept wing flutter analyses at $M=0$ and $z=0$.

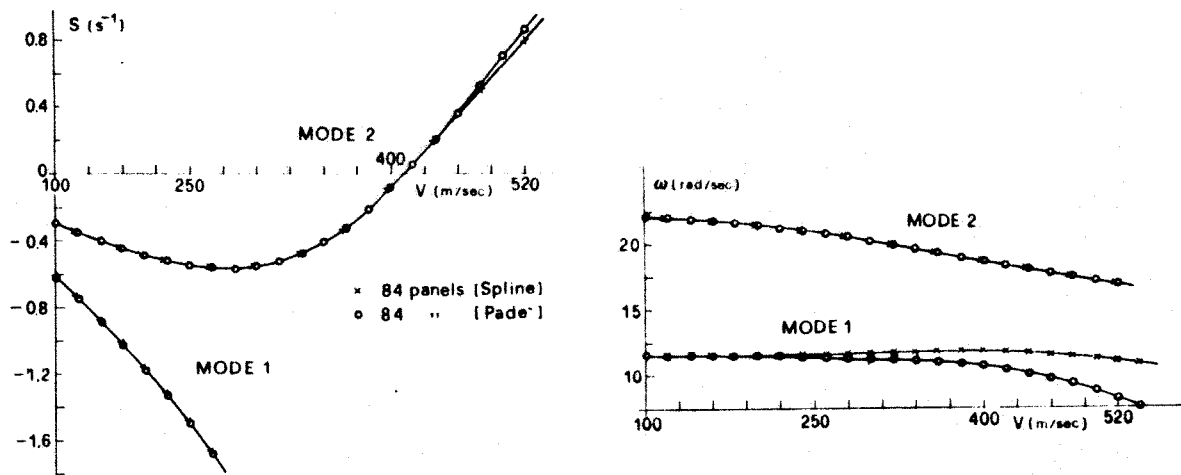


Fig.21 - Flutter modes corresponding to 84 aerodynamic panels.

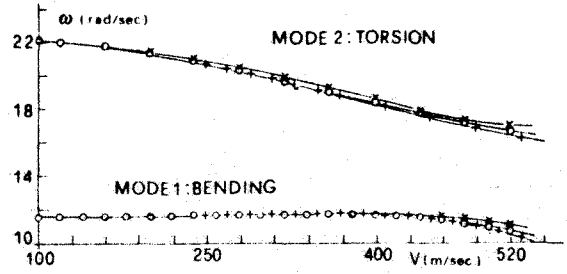
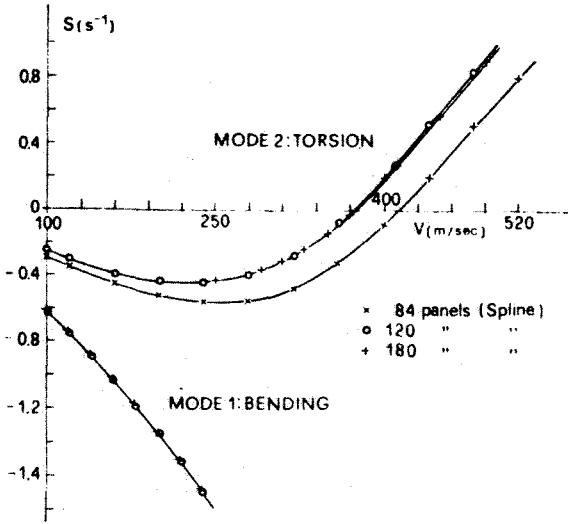


Fig.22 - Flutter modes corresponding to 120 aerodynamic panels

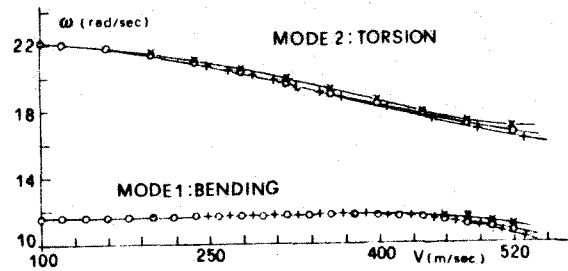
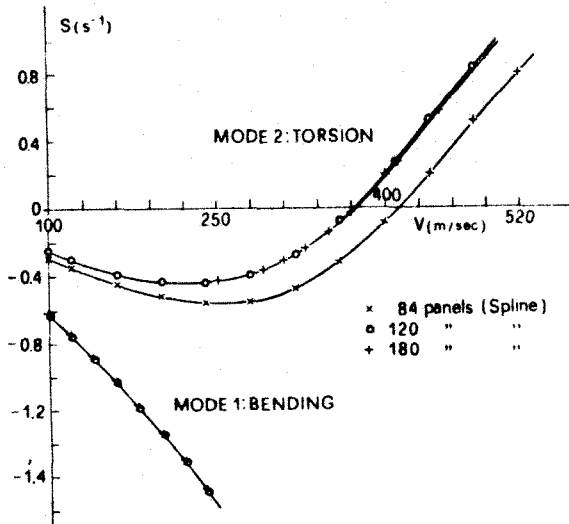


Fig.23 - Influence of aerodynamic mesh on the flutter modes.

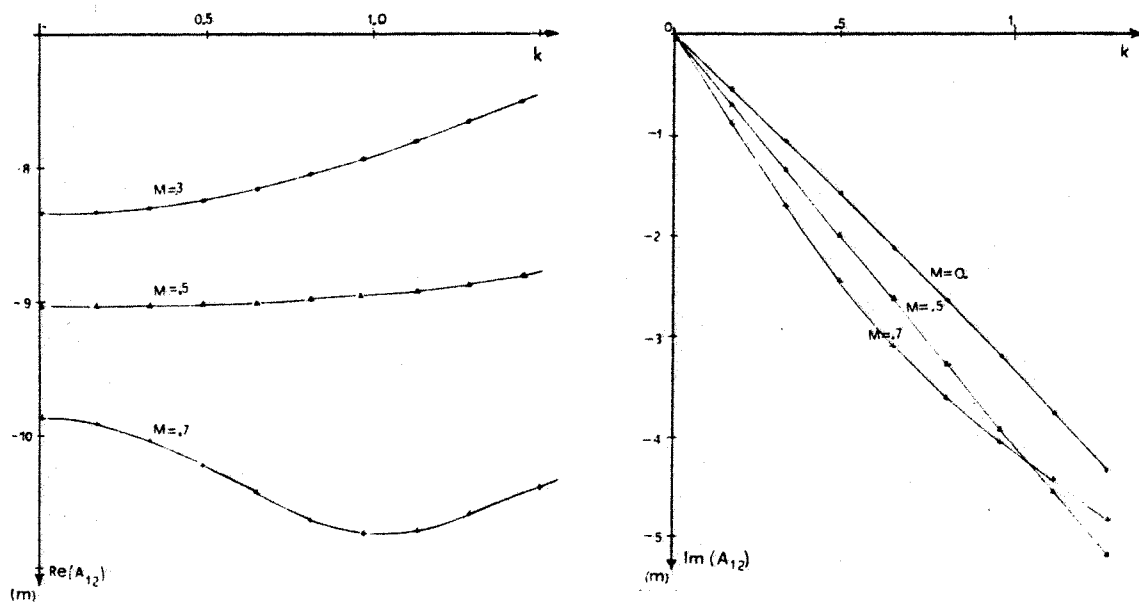


Fig.24 - Typical behaviour of aero.matrix elements vs.the reduced frequency.

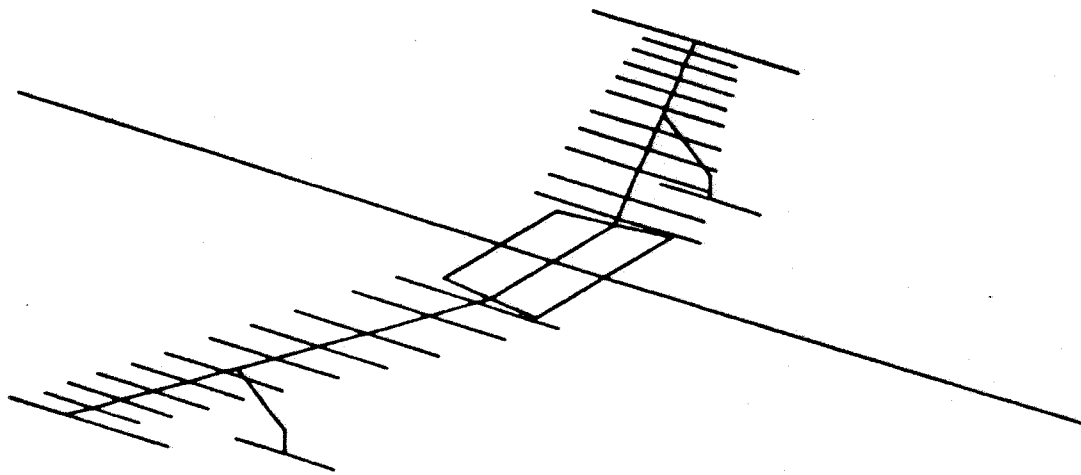


Fig.25 - Swept wing structural panel mesh; fuselage is simulated by 2 masses at a suitable distance along the airplane axis.

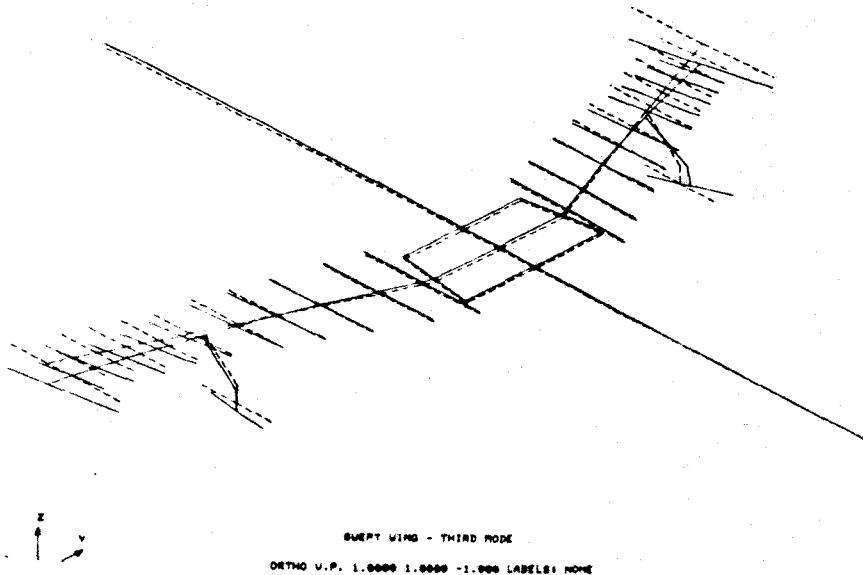


Fig.26 - A typical symmetric mode for the swept wing in fig.25.

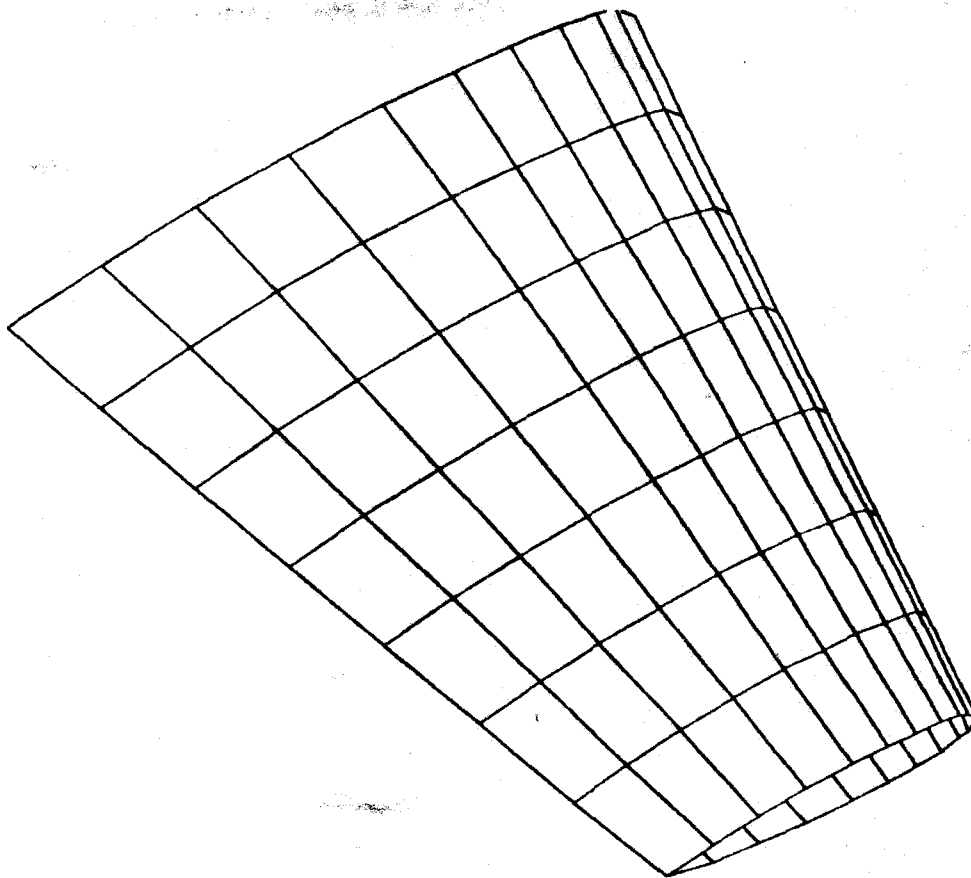
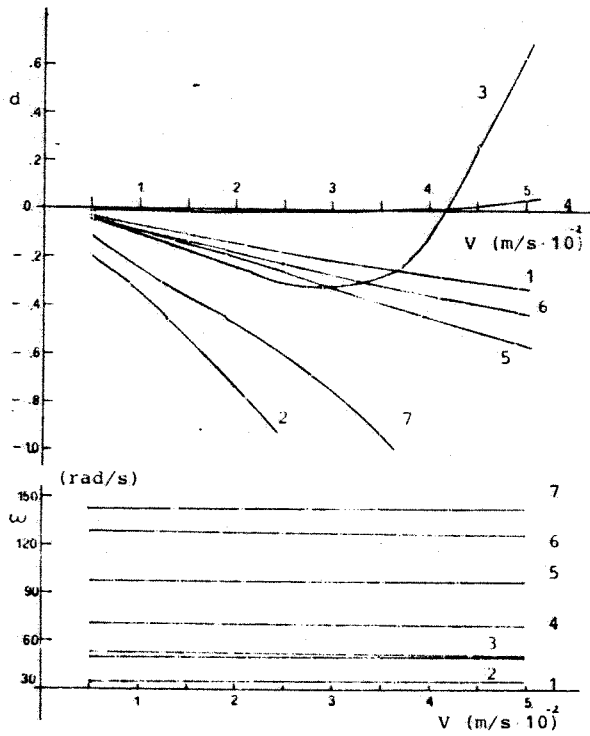
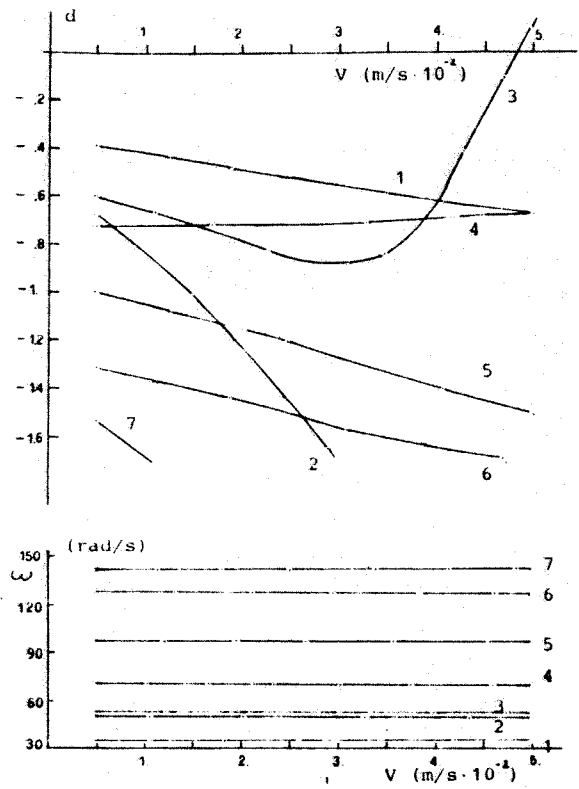


Fig.27 - Aerodynamic panel mesh for the swept wing.



a): Cubic splines,
hysteresis damping:0



b): Cubic splines,
hysteresis damping:0.02

Fig.28 - Flutter diagrams relevant to the swept wing; similar results results are obtained when the Padé approximation is used.